Biogeosciences

Open Access

Analysis of a 39-year continuous atmospheric CO_2 record from Baring Head, New Zealand

B. B. Stephens[1,2], G. W. Brailsford[1], A. J. Gomez[3], K. Riedel[1], S. E. Mikaloff Fletcher[1], S. Nichol[1], and M. Manning[3]

[1]National Institute of Water and Atmospheric Research, Wellington, New Zealand
[2]National Center for Atmospheric Research, Boulder, Colorado, USA
[3]Victoria University, Wellington, New Zealand

Correspondence to: B. B. Stephens (stephens@ucar.edu)

Abstract. We present an analysis of a 39-year record of continuous atmospheric CO_2 observations made at Baring Head, New Zealand, filtered for steady background CO_2 mole fractions during southerly wind conditions. We discuss relationships between variability in the filtered CO_2 time series and regional to global carbon cycling. Baring Head is well situated to sample air that has been isolated from terrestrial influences over the Southern Ocean, and experiences extended episodes of strong southerly winds with low CO_2 variability. The filtered Baring Head CO_2 record reveals an average seasonal cycle with amplitude of 0.95 ppm that is 13 % smaller and 3 weeks earlier in phase than that at the South Pole. Seasonal variations in a given year are sensitive to the timing and magnitude of the combined influences of Southern Ocean CO_2 fluxes and terrestrial fluxes from both hemispheres. The amplitude of the seasonal cycle varies throughout the record, but we find no significant long-term seasonal changes with respect to the South Pole. Interannual variations in CO_2 growth rate in the Baring Head record closely match the El Niño-Southern Oscillation, reflecting the global reach of CO_2 mole fraction anomalies associated with this cycle. We use atmospheric transport model results to investigate contributions to seasonal and annual-mean components of the observed CO_2 record. Long-term trends in mean gradients between Baring Head and other stations are predominately due to increases in Northern Hemisphere fossil-fuel burning and Southern Ocean CO_2 uptake, for which there remains a wide range of future estimates. We find that the postulated recent reduction in the efficiency of Southern Ocean anthropogenic CO_2 uptake, as a result of increased zonal winds, is too small to be detectable as significant differences in atmospheric CO_2 between mid to high latitude Southern Hemisphere observing stations.

1 Introduction

The future trajectory of carbon exchange between the atmosphere and the earth's oceans and terrestrial ecosystems remains a primary uncertainty in climate projections (IPCC, 2007). Predicting the response of global carbon fluxes to expected changes in atmospheric CO_2, temperature, precipitation, and surface winds requires a better understanding of how and why these fluxes vary on synoptic to decadal timescales (Friedlingstein et al., 2006; Le Quéré et al., 2007; Zickfeld et al., 2008), which in turn requires long-term, high-quality, and globally distributed observations of atmospheric CO_2 mole fractions (Keeling, 1961; Keeling et al., 2001; Rödenbeck et al., 2003; Gurney et al., 2008; Patra et al., 2008).

As the primary area for the exchange of heat and gases between recently upwelled surface waters and the atmosphere, the Southern Ocean is a region of critical importance for future climate change and atmospheric CO_2 (Sarmiento et al., 1998; Caldeira and Duffy, 2000). However, the Southern Ocean's response to climate change depends on complex interactions between biogeochemical and dynamic processes, and the net feedback on anthropogenic CO_2 uptake will be

mediated by varying influences associated with changes in solubility, biological, and anthropogenic forcing (Sarmiento et al., 1998; Caldeira and Duffy, 2000; Zickfeld et al., 2008; Lovenduski and Ito, 2009). Observations over the past several decades have suggested a significant poleward intensification and strengthening of Southern Ocean winds (Thompson and Solomon, 2002; Marshall, 2003), yet it is unclear what effect these changes are having on deep-water ventilation (Saenko et al., 2005; Böning et al., 2008) or what effect ventilation changes may be having on air-sea CO$_2$ fluxes (Wetzel et al., 2005; Le Quéré et al., 2007; Lovenduski et al., 2007; Law et al., 2008; Zickfeld et al., 2008; Lenton et al., 2009; Lovenduski and Ito, 2009; Takahashi et al., 2009).

Long-term atmospheric CO$_2$ records at mid to high southern latitudes have significant potential to shed light on past and ongoing changes in Southern Ocean CO$_2$ fluxes. However, the available records are few and regional background CO$_2$ gradients induced by changes in the Southern Ocean carbon sink are small, which makes their interpretation by atmospheric transport models challenging (Law et al., 2003; 2008). As a consequence, the available records are important and should be examined closely to improve their compatibility across the global network and to maximize their scientific utility through data-based analyses.

One of the longest CO$_2$ records comes from Baring Head, New Zealand (BHD), where continuous instruments have recorded measurements since 1972 (Lowe et al., 1979; Manning and Pohl, 1986; Manning et al., 1994; Brailsford et al., 2012) and are currently operated by staff of the New Zealand National Institute of Water and Atmospheric Research (NIWA). These data have been used in studies investigating the global carbon cycle and in community data synthesis products (e.g., Keeling et al., 1989a; Keeling et al., 2001; Gurney et al., 2002; Le Quéré et al., 2007; Globalview-CO$_2$, 2011; WDCGG, 2012). There are relatively few atmospheric CO$_2$ observing sites in the Southern Hemisphere. Other notable long-term sites include the South Pole (SPO), with flasks collected by Scripps Institution of Oceanography (SIO) since 1957 and in situ measurements by the US National Oceanic and Atmospheric Administration (NOAA) since 1976, and Cape Grim, Tasmania, with in situ measurements by the Commonwealth Scientific and Industrial Research Organisation also since 1976. Of the 17 active sites south of 30° S, only 8 record in situ CO$_2$ measurements (WDCGG, 2012). As a member of this small group, the Baring Head record is particularly valuable for addressing questions about interannual variability and trends for the carbon cycle at high southern latitudes and globally. Lowe et al. (1979) discussed the results from the first 4 yr of this dataset, describing the secular trend and seasonal cycle. Here, we present a newly reprocessed version of the full dataset and its variability with respect to other stations and important climate processes. A companion paper details the history of the site, measurement techniques, calibration methodology, and intercomparison results (Brailsford et al., 2012).

To aid interpretation of the Baring Head CO$_2$ time series and provide clues to sources of the observed trends and variability, we include measurements from the SIO CO$_2$ program made on flasks collected at the South Pole and by in situ instrumentation at Mauna Loa Observatory in Hawaii (MLO) (Keeling et al., 2001). The high time resolution of the Baring Head data allows for robust identification of background mole fractions as well as analyses of synoptic scale processes. In this paper, we focus on the interpretation of measurements that have been filtered to sample during steady CO$_2$ conditions when air is arriving from the high-latitude Southern Ocean. Aspects of the regional information contained in short-term variations will be the focus of subsequent research. In Sect. 2 we summarize the Baring Head site characteristics including information on the origins of air masses arriving at the site, the selection criteria for steady periods, and our atmospheric transport modeling methods. In Sect. 3, we analyze and discuss annual mean mole fractions, seasonal and interannual variations, and long-term trends in the CO$_2$ time series and their relationship to Southern Ocean and global carbon exchanges.

2 Background and methods

2.1 Site location and air origins

In 1970, in conjunction with the Department of Scientific and Industrial Research (DSIR, predecessor to NIWA) in New Zealand, C.D. Keeling's group from SIO established a non-dispersive infrared (NDIR) analyzer at Makara (41.2473 S, 174.6944 E) about 15 km northwest of Wellington and 1 km inland from the west coast of the North Island, New Zealand (Fig. 1a). However, the first 1.5 yr of measurements at this site suggested that it was too strongly influenced by local terrestrial signals, and the analyzer was moved to Baring Head (41.4083 S, 174.8710° E) in December, 1972. The measurements of atmospheric CO$_2$ at the Baring Head site have continued to the present, making it the longest running in situ atmospheric CO$_2$ observing station in the Southern Hemisphere and the second longest globally.

Baring Head is located approximately 10 km southeast of the city of Wellington (Fig. 1a). The measurement system is housed in a concrete building close to the edge of a coastal cliff with a southerly aspect. A pair of air intakes is located 10 m above the adjacent ground level, 85 m a. m. s. l., and approximately 240 m from the ocean. The intervening land consists of a beach strip and cliff face containing sparse, shrubby vegetation. There is a single residence to the north of the site; otherwise, there is no permanent occupation within 3 km. The surrounding land has been used fairly consistently for low density livestock farming. The Wellington city area has a population of approximately 360 000. The station is visited by NIWA staff for maintenance of equipment on a weekly schedule.
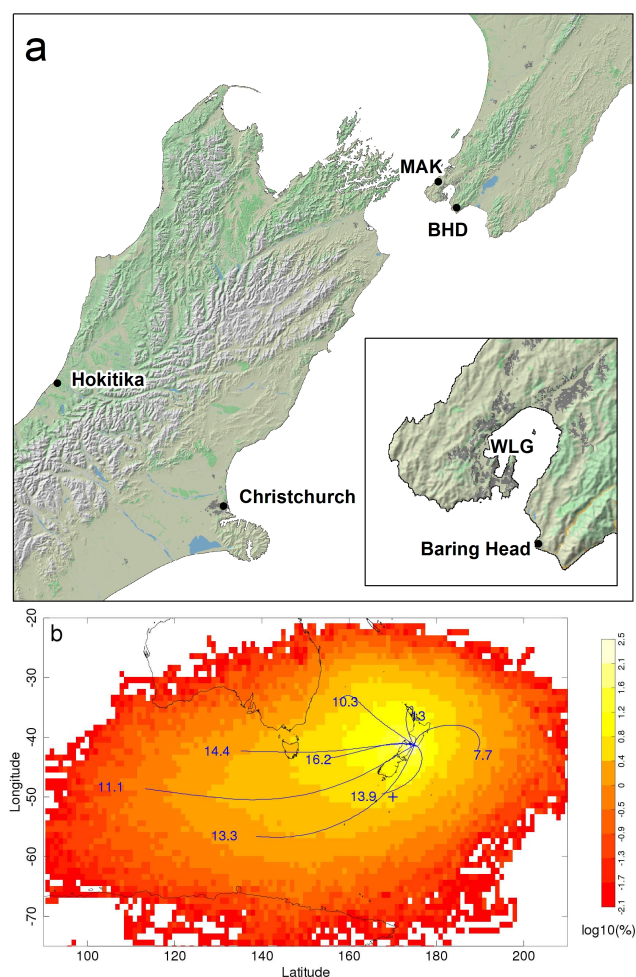
Fig. 1. Maps showing **(a)** the location of Baring Head (BHD) and other landmarks, and **(b)** clustered results of 20 yr (1988–2007) of twice-daily 4-day back-trajectory calculations, with percentages indicated for each cluster. In **(a)**, labels also indicate Makara (MAK) and Wellington (WLG) on the North Island, and colors indicate forests (green), inland water (blue), populated areas (dark gray), non-forested land (beige), and above tree line (light gray). In **(b)**, color shading indicates a logarithm of the percentage of trajectories crossing a given latitude/longitude square. The + symbol indicates the location of TM3 model output used for comparison to steady period data in order to avoid local terrestrial influences in the model.

Baring Head was chosen to make CO₂ measurements representative of large relatively homogeneous Southern Ocean air masses. Wind speeds at the site are typically high, reducing the impacts of local sources. Also, southerly air arriving at this site has often been out of contact with terrestrial sources and sinks of CO₂ for thousands of km, having travelled over the Southern Ocean between the latitudes of 45 and 70° S for the preceding week or more. These characteristics provide ideal conditions for determining background levels of atmospheric CO₂ at these latitudes, but at other times the site receives air that has recently passed over New

Zealand or Australia. Fig. 1b shows the results of a clustering analysis on 20 yr of 4-day back trajectories for air arriving at Baring Head. The back trajectories were calculated every 12 h using the method of Gordon (1986) driven by winds from the New Zealand Meteorological Service primitive equation model. The clustering was performed using a convergent k-means procedure, which is described in Kidson (1994).

Onshore winds are usually associated with a repeating synoptic pattern in which an anticyclone moves from the Tasman Sea, to the west of New Zealand, onto the country modulating the background westerly winds (Kidson, 2000). The Southern Alps of the South Island of New Zealand, which reach a height of 3750 m, have a major effect on air flow throughout the region. When the center of an anticyclone is well to the west of New Zealand, the mountain range acts to deflect air flow northward along the west coast of the South Island and then through the Cook Strait separating the North Island and the South Island. This results in a northwest wind in the strait that is further channeled by topography to a local wind at Baring Head that is from the north. Most of the back trajectories from the northwest sector in Fig. 1b correspond to local winds from the due north at Baring Head, although the model used to produce the back-trajectories does not have sufficient resolution to capture this topographic forcing. As the anticyclone moves eastward, a transition occurs to a regime in which air flows around the south of the South Island, and the local wind at Baring Head is from the south. This synoptic pattern is typically associated with a descending air mass and back trajectories that come from around 55° S and have not crossed land in at least 4 days. As the clustering analysis in Fig. 1b indicates, south and southeast arriving trajectories occur approximately 27 % of the time. Southerly wind events can persist for several days at a time and occur roughly 4 times per month in winter and 2 times per month in summer.

2.2 Data filtering

Isolating clean marine background measurements from those influenced by local terrestrial fluxes requires a data filtering scheme informed by a good knowledge of the local site and wind conditions and their influence on CO₂ variability. As discussed above, the topography of the South Island, Cook Strait, and the mountains near Baring Head result in the site almost exclusively experiencing due northerly or due southerly winds that are often quite strong. Figure 2a shows frequency distributions for winds of different directions and speed. As this Fig. indicates, approximately 2/3 of the time the hourly average wind direction is within 30 degrees of north, and 1/2 of these winds are over 10 m s⁻¹. The remaining 1/3 of the time, the wind is primarily from the south, with 2/3 of these winds over 10 m s⁻¹ and the stronger winds holding closer to due south.
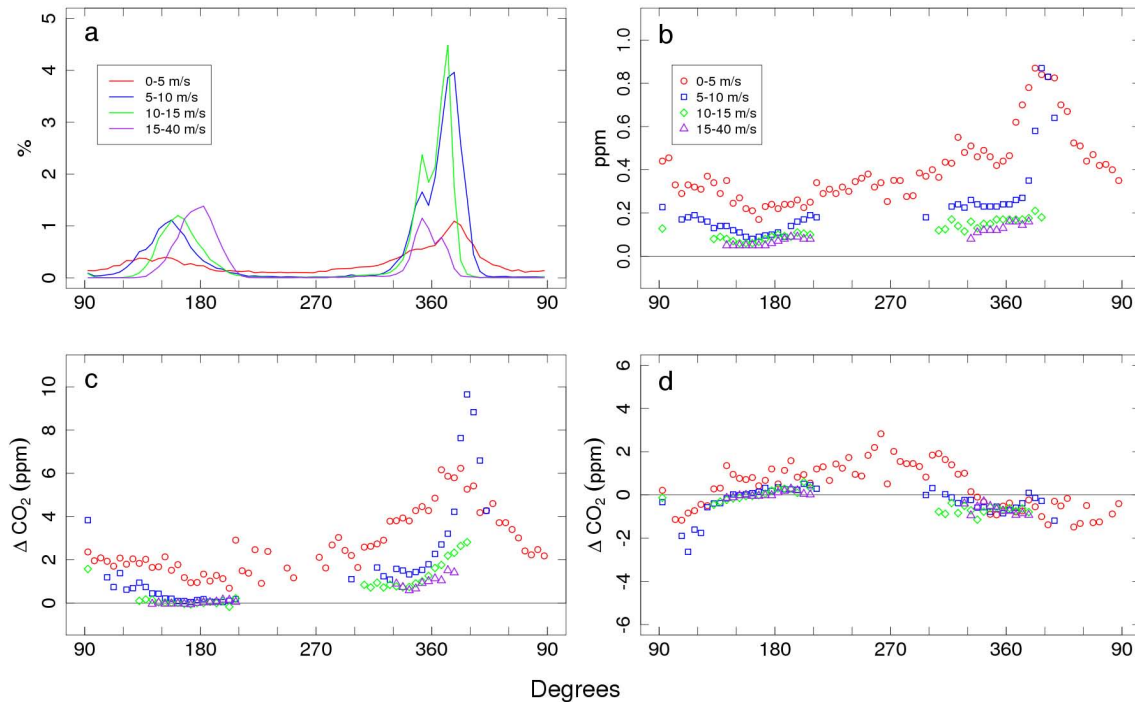
Fig. 2. Influence of wind speed and direction on CO_2 mole fractions and variability as derived from Baring Head data from 1997–2011. **(a)** Wind direction distributions for four different wind speed ranges shown as percentage of all winds in 5-degree increments. **(b)** Hourly CO_2 variability (1-sigma) as a function of wind direction for four different wind speed ranges. **(c)** Differences between nighttime (22:00–04:00 LST) hourly mean observed CO_2 mole fractions and interpolated steady period data for four different wind speed ranges. **(d)** Same as **(c)** but for daytime (10:00–16:00 LST). For **(b–d)**, points are only plotted if that wind direction and speed bin represents 0.05 % or greater of all wind conditions.

These wind conditions have a major influence on CO_2 variability, with hourly standard deviations less than 0.2 ppm corresponding to strong northerlies and moderate and strong southerlies, and higher variability to weak winds and moderate northerlies (Fig. 2b). Although strong northerlies are often associated with low CO_2 variability, it is apparent from comparing mole fractions measured during these episodes to those during southerlies that they still reflect significant terrestrial influences. Figures 2c and d show that these strong northerlies are typically 1.0–1.5 ppm higher in CO_2 during night, and 0.5–1.0 ppm lower during day as a result of upwind respiration and photosynthesis on the North Island. High daytime CO_2 mole fractions during infrequent weak westerlies likely result from emissions associated with the large populations in the city of Wellington and surrounding suburbs.

In order to obtain a baseline record representative of large marine air masses, we have employed a filter focused on retrieving long durations of steady CO_2 mole fractions when air arrived from the south without first crossing over the South Island (see Fig. 1). We start with a multi-step filter in which first "steady intervals" for either of two inlet lines are defined as intervals for which the CO_2 mole fraction has a maximum standard deviation of 0.1 ppm for a minimum
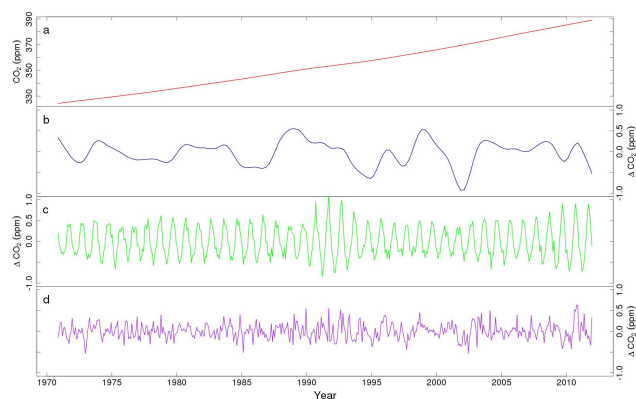
length of 6 h. Then, overlapping steady intervals for one or both inlet lines are aggregated into "steady periods", which can themselves have slowly trending mole fractions. Next, these steady periods are further screened to exclude cases when the wind was not from the south, and finally they are also screened to exclude cases when it is likely the air passed over the South Island before arriving at Baring Head. This last step is accomplished by requiring that the atmospheric pressure difference across the Southern Alps, as measured by the difference between pressure at Christchurch on the east coast and that at Hokitika on the west coast (Fig. 1a), be 1 mbar or greater averaged over the steady period (Manning and Pohl, 1986). We use the term "steady interval" to refer to a 6-plus hour span from a single inlet with 0.1 ppm or less standard deviation, and the term "steady period" to refer to a complete set of overlapping intervals, to be consistent with prior Baring Head data reports. Steady periods further filtered on meteorological conditions then represent what other investigators often call "background" or "baseline" data.

Prior to March of 1978, steady period selection was done manually on the basis of consecutive 30 min averages having a range less than 0.1 ppm, and including the southerly criteria but not the Christchurch-Hokitika pressure difference. Using the newer filter criteria over the 33 years since then, steady
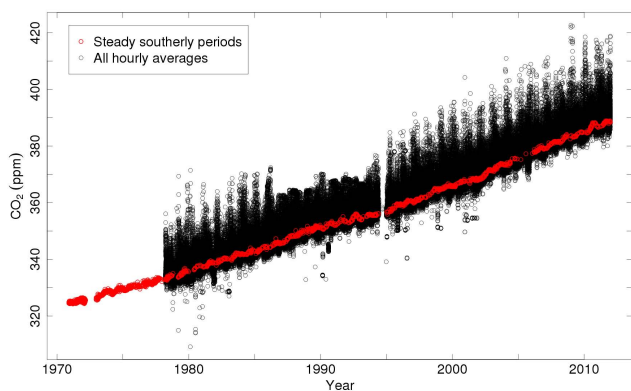
Fig. 3. Baring Head CO$_2$ time series, showing all hourly averages (black) and data filtered for steady southerly periods as described in the text (red). The filtered data are shown as average values for the entire steady period. The years from 1987–1994 with truncated hourly CO$_2$ peaks resulted from an intentional adjustment of the analyzer output range to increase sensitivity during southerly wind periods, but sacrificing measurements during locally influenced high CO$_2$ episodes. With the focus on the steady period data, the hourly average record was not historically scrutinized. Low CO$_2$ anomalies in the hourly average record prior to 2002 likely result from instrumentation problems, and work is currently underway to use handwritten notes to identify and filter such events out. Prior to 1978, high-rate measurements were recorded on strip charts, but only the steady period data are available in digital form. The plotted data prior to December 1972 are from the Makara site.

Fig. 4. Results of STL decomposition of the Baring Head steady period CO$_2$ record. **(a)** trend component found using 10-year window, **(b)** interannual component found using 2-year window, **(c)** seasonal component using a 5-year window on monthly trends, and **(d)** remainder component. For **(b–d)**, the y-axis scales are similar. The fits include data prior to December 1972 from the Makara site.

periods have been found to occur on average 36 times per year, last on average 17 h, and constitute 13 % of the complete observational record. This is significantly less than the percentage of southerly conditions because of the requirement for the conditions to persist for 6 h. There is significant seasonal variability in the occurrence of steady periods and also some in their duration, with 67 % more periods, totaling twice as much overall time, occurring in the winter months of June–August compared to the summer months of December–February. The southerly criterion excludes 13 % of steady CO$_2$ periods, but less than 8 % in terms of time as the northerly steady CO$_2$ periods tend to be shorter. The Christchurch–Hokitika pressure difference excludes another 26 % of the remaining steady periods and 18 % in terms of time. Each of the resulting filtered steady periods is treated as a unique single event, and CO$_2$ data reported to community data collections (Globalview-CO$_2$, 2011; WDCGG, 2012) have historically consisted of average mole fractions, standard deviations, start times, and durations for each steady period. Figure 3 shows both the unfiltered and filtered CO$_2$ time series for Baring Head. The smoothness of the steady period curve relative to the scatter of all hourly averages reveals the power of this filtering method to isolate remote marine signals. Simple filters based on hourly wind direction or within hour CO$_2$ variability are much less selective. The frequency of steady periods found has varied from year to year.

Although this may be the result of changes in atmospheric transport patterns or variable CO$_2$ fluxes, variations in the number of steady periods could also be related to changes in instrument procedures or performance (Brailsford et al., 2012).

We employ the detailed filter criteria to enable time-series analysis on low-variability background marine air and to investigate questions about changes in Southern Ocean fluxes. Coarse-resolution models that use these filtered steady period Baring Head data or synthesized products based on them (Globalview-CO$_2$, 2011) must account for this filtering to adequately represent the observing conditions. Recognizing the ability of more recent models to combine higher resolution data with information on corresponding synoptic transport in order to infer fluxes on regional scales, we also make the hourly mean unfiltered CO$_2$ time series publicly available, along with values for short-term variability and winds.

2.3 Atmospheric transport modeling

To aid in interpreting the observations at Baring Head, we have used simulations from the fine grid version of the Transport Model version 3 (TM3) (Heimann and Körner, 2003), which has a resolution of $\sim 3.8°$ latitude by 5° longitude with 19 vertical levels. TM3 is a three-dimensional Eulerian model driven by off-line winds from the NCEP reanalysis (Kalnay et al., 1996). TM3 has been included in several model intercomparison studies (e.g., Gurney et al., 2002; Gurney et al., 2003; Baker et al., 2006).

We used the CO$_2$ sources and sinks from the Carbon-Tracker 2010 data assimilation product (Peters et al., 2007) as boundary conditions for the model. The model simulations were run from 2000–2009, and the first 3 yr of these simulations were removed to account for model spin-up. In order to
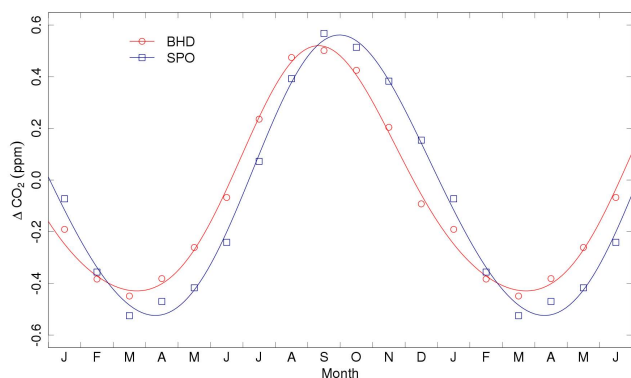
Fig. 5. Long-term average Baring Head and South Pole seasonal CO₂ cycles shown as monthly means of the STL fit seasonal component (symbols) along with 2-harmonic fits to detrended monthly mean data (lines). 18 months are shown with Jan–Jun repeated for clarity.

be able to isolate the influence of different regions and source processes on the station, CO_2 from fossil-fuel emissions, biomass burning, the terrestrial biosphere, and the oceans were each treated as separate tracers in the model and separated geographically according to the TransCom flux regions (Gurney et al., 2003). To determine the modeled sensitivity at a particular station to a particular source, we divide the corresponding CO_2 signal, averaged over the years 2003–2009, by the corresponding source strength. The resulting sensitivities are similar to those found with other atmospheric transport models (Gurney et al., 2003). For our calculations, we extract CO_2 values at a point 1000 km to the southwest of Baring Head (50° S, 170° E; see Fig. 1) to represent the filtered steady period Baring Head record, as the modeled values for Baring Head used no filtering for steady-CO_2 southerly wind conditions. The selection of this point is somewhat arbitrary, but avoids local terrestrial influences and is close to the two southerly back-trajectory clusters (Fig. 1b).

3 Results and discussion

3.1 Time series

Salient features of the long-term filtered steady period record include (1) a long-term growth rate of approximately 1.5 ppm yr^{-1} driven by global fossil-fuel consumption and deforestation, (2) annual-mean differences with respect to other stations consistent with fossil-fuel burning in the Northern Hemisphere and oceanic CO_2 uptake in the Southern Hemisphere, (3) a seasonal cycle of around 1 ppm amplitude related to ocean exchange in the Southern Hemisphere and the influence of terrestrial fluxes in both the Northern Hemisphere and Southern Hemisphere, (4) interannual variations in the long-term growth rate reflecting global and Southern Ocean carbon cycle processes, and (5) long-

term trends in differences from other stations, which have the potential to constrain trends in Southern Ocean CO_2 fluxes.

To visually decompose the variations on different time scales, we use the seasonal time-series decomposition by Loess (STL) routine (Cleveland and McRae, 1989; Cleveland et al., 1990), which allows for changes in seasonal patterns over time. This routine fits locally weighted polynomial regressions to time series composed of all values from individual months, for example all average January values for the entire record, as well as the remaining deseasonalized trend, in an iterative process. The degrees to which the seasonal cycle and long-term trend are allowed to vary to fit the data are set by specifying the window for the seasonal and trend Loess fits. We use a seasonal cycle window of 5 yr and first run the procedure using a trend window of 121 months intended to reflect changes on decadal timescales. Then, after removing this component we run the procedure again with a trend window of 25 months to capture subdecadal components. Figure 4 shows the results of this STL calculation for Baring Head. We have run the same routine and parameters on South Pole flask and Mauna Loa continuous data from SIO for the overlapping years.

3.2 Annual-mean mole fractions

As shown in Table 1, the average difference over the entire 39-year record between Baring Head and Mauna Loa (BHD–MLO) is –2.30 ppm, and between Baring Head and the South Pole (BHD–SPO) is +0.05 ppm. For the decade 2000–2009, the average BHD–MLO difference is –3.03 ppm and the average BHD–SPO difference is –0.05 ppm, opposite in sign to that for the full record. The Baring Head record exhibits increasingly lower mole fractions than the Mauna Loa record because of the predominance and growth of fossil-fuel CO_2 emissions in the Northern Hemisphere and oceanic CO_2 uptake in the Southern Hemisphere. Despite being further north than the South Pole, Baring Head shows similar and trending lower annual-mean CO_2 mole fractions. This reflects the greater influence of the increasing Southern Ocean CO_2 sink on air at Baring Head (Keeling et al., 1989b, Kawa et al., 2004).

The TM3 model sensitivities (Sect. 2.3) scaled by 2000–2009 fossil fuel CO_2 sources (Boden et al., 2009, as extrapolated by CarbonTracker 2010) result in an average BHD–MLO difference of –4.57 ppm and an average BHD–SPO difference of 0.17 ppm (Table 1). The TM3 model sensitivities suggests that a postulated 0.3 Pg C yr^{-1} sink in the high-latitude Southern Ocean (Gruber et al., 2009) results in a –0.38 ppm BHD–MLO difference and a –0.13 ppm BHD–SPO difference. Furthermore, the model sensitivities predict that a plausible 1.1 Pg C yr^{-1} sink in the temperate Southern Hemisphere oceans (Gruber et al., 2009) results in a –0.87 ppm BHD–MLO difference and a –0.07 ppm BHD–SPO difference. Although southern temperate ocean fluxes have relatively small influences on the annual mean

Table 1. Observed and modeled intersite CO_2 differences (ppm).

	BHD – MLO	BHD – SPO
Observed 1972–2011	–2.30	+0.05
Observed 2000–2009	–3.03	–0.05
TM5 atmospheric transport model[a]		
2000–2009 fossil fuel source	–4.57	+0.17
$0.3 \, \text{Pg C yr}^{-1}$ high-latitude Southern Ocean sink	–0.38	–0.13
$1.1 \, \text{Pg C yr}^{-1}$ Southern Hemisphere temperate ocean sink	–0.87	–0.07
Residual difference (fossil + ocean – observed)[b]	+2.79	+0.02
$-0.2 \, \text{Pg C yr}^{-1}$ change in Southern Ocean sink over 1968–2005	–0.25	–0.09
$+0.1 \, \text{Pg C yr}^{-1}$ change in Southern Ocean sink over 1985–2005	+0.13	+0.04
Le Quéré et al. (2007) observed winds vs. constant winds[c]	+0.11	+0.05

[a] Differences shown are for (50° S, 170° E) – MLO and (50° S, 170° E) – SPO to represent filtered steady southerly period selection of BHD data, as described in the text.
[b] To the extent that the two nominal ocean sinks are correct, this represents the combined influence of tropical and Northern Hemisphere land and ocean CO_2 exchange.
[c] Differences shown are for MQA – MLO and MQA – SPO to represent steady southerly period selection of BHD data, as described in the text.

BHD–SPO differences, because atmospheric transport generates phase differences, they can have a larger effect on monthly site differences. Tropical and Northern Hemisphere terrestrial biosphere and ocean fluxes are responsible for countering the influence of the fossil-fuel source and Southern Ocean sink on the BHD–MLO gradient, to produce the observed value (Table 1), but their relative proportion is model-dependent and a topic of active research (Stephens et al., 2007). TM3 and other models suggest that tropical and northern fluxes have little influence on the BHD–SPO differences. The counteraction of the fossil-fuel source and Southern Ocean sinks described above can explain the observed 2000–2009 annual-mean BHD–SPO difference well within the limits of uncertainty (Table 1).
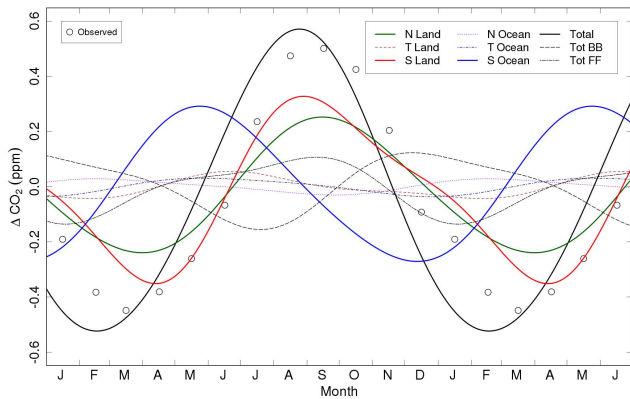
3.3 Seasonal cycles

Figure 5 shows the average seasonal cycles at Baring Head, for filtered steady period data, and at South Pole for the 39 yr of the Baring Head record. The amplitude of the average Baring Head cycle is 0.95 ppm with a late-winter maximum in September, and an autumn minimum in March. This cycle is 13 % smaller and 3 weeks earlier in phase compared to that at the South Pole. Both cycles are small relative to those at Northern Hemisphere stations, but their timing and amplitudes may represent important tests for our understanding of hemispheric CO_2 fluxes and interhemispheric atmospheric transport (Dargaville et al., 2003; Baker et al., 2006).

Early studies recognized that seasonal cycles in atmospheric CO_2 at high southern latitudes represented the combined influences of Northern Hemisphere terrestrial fluxes delayed by interhemispheric transport and Southern Hemisphere terrestrial and oceanic fluxes (Pearman and Hyson, 1980; Heimann and Keeling, 1989) but lacked sophisticated estimates of these processes. More recent models of atmospheric CO_2 at high southern latitudes incorporate improved knowledge of flux distributions and better transport, but still show differences in relative seasonal contributions at high southern latitudes (Erickson et al., 1996; Heimann et al., 1998; Dargaville et al., 2002; Roy et al., 2003; Gurney et al., 2004; Nevison et al., 2008; Takahashi et al., 2009). However, the general picture for the Baring Head record has remained relatively consistent over time, in which the influence from Northern Hemisphere terrestrial fluxes is lagged by approximately 6 months and reduced such that it is comparable in phase and magnitude to that from Southern Hemisphere terrestrial fluxes (Heimann and Keeling, 1989; Heimann et al., 1998).
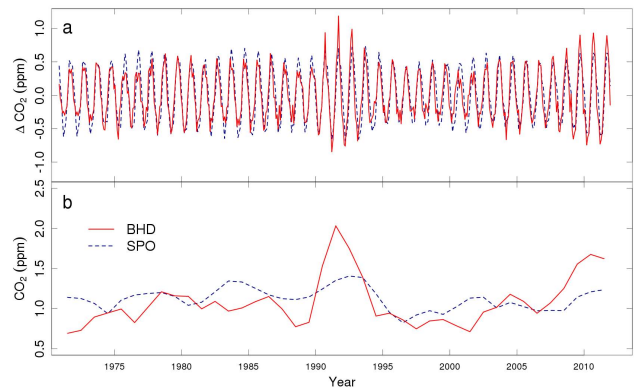
Figure 6 shows model-estimated contributions to the seasonal CO_2 cycle from various sources for the simulated point to the southwest of Baring Head. These curves were obtained by fitting the CarbonTracker/TM3 model output for the years 2003–2009 with 2-harmonic seasonal cycles. The Northern Hemisphere and Southern Hemisphere terrestrial influences both have peaks in late austral winter (August–September) and troughs in austral autumn (March–April). The Southern Hemisphere ocean contribution has a peak in late austral autumn (May) and trough in early austral summer (December), comparable in magnitude and leading by around 5 months the Northern Hemisphere and Southern Hemisphere terrestrial influences, and reflecting thermal forcing at lower latitudes rather than biological forcing at high latitudes (Heimann et al., 1998; Takahashi et al., 2009). The combination of these out-of-phase influences leads to a modeled Baring Head peak in atmospheric CO_2 in austral winter (August) and trough in austral summer (February). This model cycle is comparable in magnitude to the observations but is one month advanced in phase.

Fig. 6. Contributions to the seasonal CO_2 cycle at Baring Head as simulated by TM3 forced by CarbonTracker 2010 fluxes (Peters et al., 2007). 18 months are shown with Jan–Jun repeated for clarity. The northern (N), tropical (T), and southern (S) allocations are based on the TransCom regions (Gurney et al., 2003) with tropical divisions at approximately 15° N and 15° S. Total contributions from biomass burning (BB) and fossil-fuel emissions (FF) are also shown. The observed cycle from Fig. 5 is plotted again here for comparison to the total model curve.

Fig. 7. (a) Seasonal CO_2 cycle components from STL decomposition of Baring Head and South Pole records. Fits used a 5-year smoothing window on Loess fits to individual monthly time series. The BHD line is the same as that shown in Fig. 4c. **(b)** Seasonal CO_2 cycle peak-to-peak amplitudes from curves in **(a)**. The fits include data prior to December 1972 from the Makara site.

In the model, both the oceanic and terrestrial contributions to the atmospheric CO_2 seasonal cycle are advanced in phase at Baring Head relative to the South Pole (not shown), which reflects the mixing time needed for signals to propagate from further north and explains the resulting phase difference between these two stations. The modeled Southern Ocean contribution is larger in amplitude at Baring Head than at South Pole. In the real atmosphere, this may result in a greater cancellation of the out-of-phase terrestrial contribution, potentially explaining why the observed overall amplitude is lower at Baring Head than at the South Pole. However, our model simulations produce greater seasonal amplitude at Baring Head than both observed and modeled for South Pole. This highlights the sensitivity of the seasonal cycle at Baring Head to subtle shifts in timing and magnitude of the contributing influences, and suggests that further work to characterize the influence of interhemispheric transport on seasonal CO_2 cycles in the Southern Hemisphere would be useful.

Because the resulting seasonal cycle is a delicate balance between multiple processes, it varies considerably from year to year, and can be hard to detect in some years (Fig. 3). Fig. 7 shows the interannually varying 5-year-smoothed seasonal components from STL fits to both Baring Head and South Pole, as well as the peak-to-peak amplitudes of these components. The amplitudes show some similarities, and in particular both sites show an increase in amplitude over the last 3 yr of the records, indicating that seasonal CO_2 variations are often consistent over large areas of the high southern latitudes. However, there are notable exceptions such as the large increase in amplitude at Baring Head in the early 1990s that was less pronounced at the South Pole.

Any long-term changes in seasonal amplitude or phase at Baring Head might provide clues to trends in seasonal exchange processes. Because so much of the seasonal forcing at Baring Head comes from further to the north, these changes cannot be uniquely attributed to changes at high southern latitudes. However, by differencing the seasonal variations at Baring Head and South Pole, it might be possible to isolate the influence of Southern Hemisphere ocean fluxes, as changes in northern fluxes or interhemispheric exchange times are likely to affect both stations similarly. Figure 8 shows differences between monthly means from the Baring Head filtered steady period record and South Pole. Also shown are linear trend lines fit to early summer (November–January) and early winter (April–June) months, when the modeled influence of Southern Ocean fluxes at Baring Head is maximized. Based on hypothesized changes in the upwelling-driven outgassing of CO_2 in the Southern Ocean (Le Quéré et al., 2007), we might expect to see different trends in the BHD–SPO gradient in different seasons. There are no apparent differences in the summer and winter trends shown in Fig. 8, suggesting that any changes in the seasonal aspects of Southern Ocean CO_2 change are too small to be detected by this metric.

3.4 Interannual variations

The global carbon cycle and atmospheric CO_2 mole fractions vary considerably on interannual time scales (Figs. 4 and 9). Bacastow (1976) first recognized the El Niño-Southern Oscillation (ENSO) as a dominant forcing of these changes, and numerous studies have since refined our understanding of the mechanisms involved (Keeling et al., 1989a; Jones et al., 2001; Page et al., 2002; Reichenau and Esser, 2003; Hashimoto et al., 2004; Zeng et al., 2005). Positive ENSO conditions are associated with warmer and drier conditions
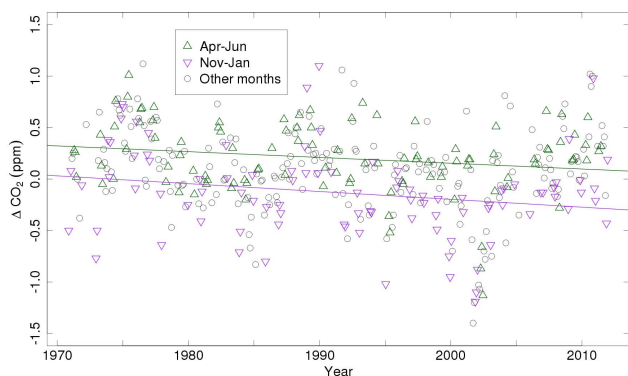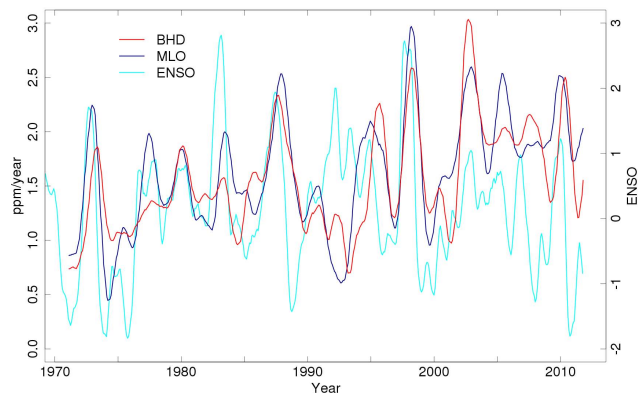
Fig. 8. Monthly mean CO_2 differences between Baring Head and South Pole. Months during the peak (April–June, green) and trough (November–January, purple) of the modeled influence from Southern Ocean fluxes (Fig. 6) are highlighted and fit with trend lines. The points prior to December 1972 are from the Makara site.

Fig. 9. Baring Head and Mauna Loa CO_2 growth rate and the Multivariate ENSO Index (Wolter and Timlin, 1993). The growth rates were calculated from the month-to-month change in the sum of the trend and interannual components of the STL fits to each record (Fig. 4a and b for BHD). All three time series have been smoothed with a 5-month running mean for clarity. The fits include data prior to December 1972 from the Makara site.

on land, leading to decreased photosynthesis and increased respiration and fire activity, while a smaller ocean response in the opposite direction results from less outgassing of CO_2 from upwelled waters in the tropical Pacific (Feely et al., 1999; Zeng et al., 2005). The net result for atmospheric CO_2 mole fractions is a positive correlation between CO_2 growth rate and ENSO, with CO_2 growth rate lagging ENSO by around 5 months. Terrestrial carbon exchange also responds on similar timescales to large-scale temperature fluctuations not directly related to ENSO (Keeling et al., 2001).

As Fig. 9 shows, the interannual fluctuations in CO_2 growth rate at Baring Head are very similar to those at Mauna Loa, and both are closely related to the ENSO cycle. The high CO_2 growth rates in the Baring Head record in 1973, 1979, 1983, 1987, 1998, 2002, and 2010 are all associated with leading El Niño events. Although the upward response at BHD to one of the strongest El Niños in 1983 is less than at MLO, it is possible that other factors led to an increased growth rate at Baring Head the year prior to the El Niño, obscuring the signal. The overall similarity to Mauna Loa highlights the global reach of the atmospheric CO_2 variations in response to ENSO. As estimated by correlation coefficients, ENSO can explain 23 % of the variability in the interannual component of the Mauna Loa STL fit at an optimal lag of 4 months, and can explain 16 % of the variability in the interannual component of the Baring Head STL fit at an optimal lag of 6 months. The peak in Mauna Loa growth rate in 1994–1995 is an example of warm global temperatures not associated with El Niño (Keeling et al., 2001), though it is only partially matched by a Baring Head excursion in 1995.

Another important interannual forcing agent is the occurrence of large volcanic eruptions, which have been shown to lead to global cooling and less respiration, as well as increased photosynthesis from more diffuse radiation as a result of aerosol scattering (Gu et al., 2002; Reichenau and

Esser, 2003; Mercado et al., 2009). These volcanic effects tend to mask or interrupt the otherwise tight connection to ENSO. For example, the extended weak El Niño that started in 1991 did not lead to positive CO_2 growth rate anomalies because of the counteracting effects of the Mt. Pinatubo eruption in June 1991 (Gu et al., 2002; Reichenau and Esser, 2003).

Interannual differences between Baring Head and Mauna Loa could result from unique ENSO forcing at high southern latitudes, different mole fraction responses to tropical forcing in the Northern Hemisphere versus Southern Hemisphere, or unrelated phenomena. Previous studies (Le Quéré et al., 2003; Verdy et al., 2007) have found evidence that the influence of ENSO events can propagate into the Southern Ocean and lead to stronger westerlies, greater entrainment of deep water, and anomalous carbon outgassing. The extent to which ENSO influences the Southern Ocean varies, and this could explain some of the differences seen between Baring Head and Mauna Loa in Fig. 9. However, the 1986–1987 El Niño had less influence on the Southern Ocean (Le Quéré et al., 2003), while the Baring Head record appears to respond similarly to Mauna Loa in this event. An additional consideration in the case of Baring Head is that El Niño influences on local wind patterns could affect the number or character of steady periods selected by the data filter (Mullan, 1996). However, we find no correlation between the number of steady periods and ENSO on monthly or yearly time scales..

Another important source of interannual variability at high southern latitudes is the occurrence of large-scale wind changes associated with the Southern Annular Mode (SAM, Hall and Visbeck, 2002). Positive phases of SAM are associated with increased westerlies in the Antarctic frontal zone, increased northward Ekman flow, and increased upwelling of
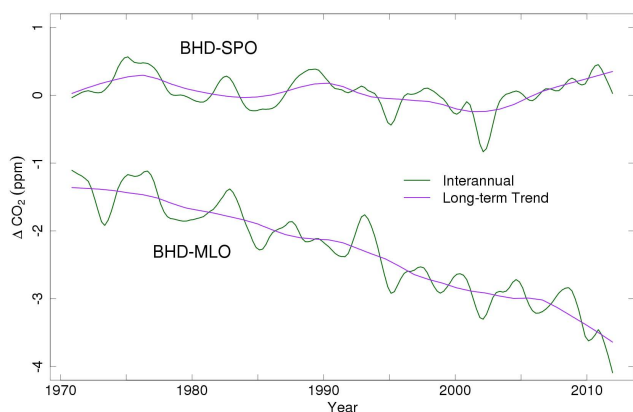
Fig. 10. BHD–SPO (top) and BHD–MLO (bottom) CO₂ differences in the interannual and trend components of the STL decomposition of the Baring Head, South Pole, and Mauna Loa records. The window for the trend fits was 10 yr, and for the interannual fits was 2 yr. The fits include data prior to December 1972 from the Makara site.

CO₂-rich water around Antarctica. Ocean biogeochemistry models (Lenton and Matear, 2007; Lovenduski et al., 2007) and atmospheric inverse models (Butler et al., 2007) suggest anomalous Southern Ocean CO₂ outgassing of around 0.1 Pg C yr⁻¹ per standard deviation of SAM. Butler et al. (2007) were able to identify signals in atmospheric CO₂ potentially associated with these flux changes by correlating month-to-month tendencies in CO₂ to the SAM index. The correlations were greatest at Palmer Station Antarctica (PSA), and decreased further from the high-latitude Southern Ocean. We have repeated the Butler et al. (2007) analysis on our Baring Head data and found no significant correlation. This could either be because the postulated high-latitude Southern Ocean flux changes have a greater impact at PSA than they do at Baring Head, or, as discussed by Butler et al. (2007), the correlation at PSA could result from local changes in wind direction that are different at Baring Head. The significant increase in seasonal amplitude (Fig. 7) then decrease in long-term growth rate (Fig. 3) from 1991–1994 in the Baring Head record could be associated with the Mt. Pinatubo eruption as discussed above, but could also be related to a negative excursion in SAM that occurred from 1991–1993. Further research on possible mechanisms driving these CO₂ changes is warranted.

Figure 10 shows the difference between the interannual and trend components of the Baring Head and Mauna Loa STL fits, and the difference between the interannual and trend components of the Baring Head and South Pole STL fits. Overall levels of interannual variability for high-latitude Southern Ocean carbon fluxes based on observational and modeling studies are on the order of ± 0.15 Pg C yr⁻¹ (1 sigma) (Louanchi and Hoppema, 2000; Le Quéré et al., 2003; Butler et al., 2007; Lenton and Matear, 2007; Lovenduski et al., 2007). Based on our TM3 sensitivities, we would expect

this to appear in the BHD–MLO difference at the ± 0.2 ppm level and the BHD–SPO difference at the ± 0.05 ppm level. From Fig. 10, it is apparent that other processes such as lower latitude Southern Ocean fluxes, Northern Hemisphere processes combined with interhemispheric transport variability, or measurement or data-filtering biases must lead to the larger interannual variations of ± 0.3 to 0.5 ppm. Similarities in the interannual BHD–MLO and BHD–SPO differences indicate times when the BHD record is most likely producing the variations.

3.5 Long-term trends

Despite the fact that year-to-year variations in Southern Ocean CO₂ fluxes have relatively small impacts on year-to-year atmospheric CO₂ gradients, long-term trends in Southern Ocean carbon exchange can have major impacts on future global atmospheric CO₂ mole fractions. Because of the large exchanges of heat and gases that occur between the atmosphere and deep ocean waters at high southern latitudes, carbon fluxes in the Southern Ocean have long been recognized as a dominant factor in determining the ocean's uptake of anthropogenic CO₂ (Knox and McElroy, 1984; Siegenthaler and Wenk, 1984; and Sarmiento and Toggweiler, 1984; Sarmiento et al., 1998; Caldeira and Duffy, 2000). CO₂ fluxes in this region are currently a sensitive balance between opposing thermal and biologic forcing (Sarmiento et al., 1998), and their response to climate change is likely to be a complex combination of dynamic effects on opposing natural and anthropogenic fluxes (Le Quéré et al., 2007; Lenton and Matear, 2007; Lovenduski et al., 2007; Zickfeld et al., 2008, Lenton et al., 2009; Lovenduski and Ito, 2009). Uncertainties in the future behavior of the global ocean carbon cycle as a whole lead to predictions with a range of 4 Pg C yr⁻¹ in 2050 (Friedlingstein, et al., 2006), with a large contribution to this range presumably coming from the Southern Ocean.

For these reasons, much effort has recently gone into investigating whether and in what direction high-latitude Southern Ocean carbon exchanges are already responding to anthropogenic forcing. Evidence suggests that, as a result of ozone depletion and climate change, Antarctic circumpolar winds have increased over the past several decades and will continue to increase in the future (Thompson and Solomon, 2002; Marshall, 2003). While it is still unclear what effect these changes are having on deep-water ventilation (Saenko et al., 2005; Böning et al., 2008), it is also unclear what effect potential changes in ventilation would have on carbon cycling. Le Quéré et al. (2007) suggested that the ongoing wind changes have increased the upwelling of carbon-rich deep waters and the outgassing of natural CO₂ from the Southern Ocean. They presented evidence from a biologic ocean model and a set of atmospheric inversions that the rate of increase in Southern Ocean carbon uptake has slowed over the past decade, resulting in a smaller uptake in proportion to the

increasing atmospheric burden. This result is consistent with long-term trends in high-latitude Southern Ocean pCO$_2$ data (Takahashi et al., 2009; Metzl, 2009) showing a faster CO$_2$ increase in surface waters than in the atmosphere. However, the result remains controversial. Law et al. (2008) argued that concerns about data quality prevents obtaining robust trends, and Zickfeld et al. (2008) showed results from a different ocean model that indicated increased overturning has led to greater uptake of anthropogenic carbon in the Southern Ocean, associated with the sinking of northward flowing surface waters.

An hourly mean version of the Baring Head record was used along with analyzed winds in the atmospheric inversion of Le Quéré et al. (2007), so we are not in a position to independently assess their result. However, it is useful to investigate what aspects of the atmospheric data may be driving the inverse result and ask how large the expected trend signals are with respect to natural variability, and how robust the attribution of trends is with respect to other natural influences and potential measurement biases. The long-term trend in the BHD–SPO difference, shown in Fig. 10, is fairly constant from 1978–2000, but there is a suggestion of a slight increase at Baring Head relative to South Pole of around 0.3 ppm over the last 10 yr of the record.

As shown in Table 1, the expected changes in atmospheric CO$_2$ gradients from the Le Quéré et al. (2007) study are quite small. Scaling the 0.2 Pg C yr^{-1} expected increase in uptake from 1968–2005 by the TM3 sensitivities only gives a –0.09 ppm expected shift in the atmospheric BHD–SPO gradient over this time. Furthermore, the proposed leveling off in this trend and decreasing efficiency of anthropogenic uptake, by about 0.1 Pg C yr^{-1} from 1985–2005, amounts to a BHD–SPO signal of only +0.04 ppm over 20 yr. This estimate is in general agreement with the actual combination of ocean and atmosphere models used by Le Quéré et al. (2007), which produce a change between Macquarie Island (MQA, 54°30′ S, 158°57′ E) and South Pole associated with the reduced deep-water upwelling of +0.05 ppm from 1985–2005 (Table 1). This number was obtained by comparing model time series (C. Rödenbeck personal communication, 2010) for Macquarie Island and South Pole for both the constant and observed wind simulations. We used model output at Macquarie Island instead of Baring Head, because the output is not selected for steady-CO$_2$ southerly wind conditions. Such small changes over 20 yr are unlikely to be detectable in comparing any two individual atmospheric CO$_2$ records. The suggestion in the observations of a +0.3 ppm change since 2001 could reflect an even larger change in Southern Ocean fluxes than modeled by Le Quéré et al. (2007), but this change is not statistically robust with respect to potential measurement biases of up to 0.3 ppm (Brailsford et al., 2012). However, this change is also coincident with a larger decrease in the BHD–MLO gradient (Fig. 10), and an even larger increase in the MLO–SPO gradient (not shown), indi-

cating that the shift in trends is global in scale and not unique to the Baring Head record.

More generally, the trends in the BHD–MLO differences in Fig. 10 are consistent with increasing fossil-fuel emissions in the Northern Hemisphere and increasing uptake of anthropogenic CO$_2$ in the mid and high latitude Southern Hemisphere oceans in response to those emissions. Notably, the rate of increase in this difference does not appear to slow since 2000. The expected change associated with increases in fossil-fuel emissions over the 39-year record (Boden et al., 2009), obtained by scaling the TM3 sensitivities discussed above, is a –2.8 ppm change in the BHD–MLO difference, which would be reduced in magnitude by increased northern terrestrial sinks but made more negative by increased Southern Ocean sinks over the same time. For BHD–MLO, scaling the ocean fluxes modeled by Le Quéré et al. (2007) by our TM3 results suggests a −0.25 ppm change due to a long-term 0.2 Pg C yr^{-1} increase in Southern Ocean CO$_2$ uptake, and a +0.13 ppm change associated with the proposed leveling off of the uptake trend from 1985–2005 (Table 1). Again, the actual combination of ocean and atmosphere models used by Le Quéré et al. (2007) agrees with this scaling, giving a change of +0.11 ppm for MQA–MLO from 1985–2005 (Christian Rödenbeck, personal communication, 2010). The expected change in BHD–MLO associated with the Southern Ocean is larger than that for BHD–SPO, but again is small with respect to natural variability, and with respect to compatibility estimates for the measurements.

In practical terms, given the number of stations used, the complexity of atmospheric transport, and the complex nature of the inversion process, it can be very difficult to determine exactly what drives a particular atmospheric inversion result (Rödenbeck et al., 2003; Gurney et al., 2004; Stephens et al., 2007). More work is needed in connection with atmospheric inverse models to trace results to quantitative features of the data so that they can be assessed in terms of potential data biases (Law et al., 2008). In addition, given that potential systematic biases between individual CO$_2$ station records and different CO$_2$ measuring laboratories are still significant (WMO, 2011; 2012), sensitivity studies should be conducted in which mole fractions at individual stations are offset by several tenths of ppm over various time frames to assess the robustness of the inversion results (Rödenbeck et al., 2006; Law et al., 2008; Masarie et al., 2011).

4 Conclusions

We have presented an analysis of a newly reprocessed version of the 39-year continuous atmospheric CO$_2$ record from Baring Head, New Zealand. This record is the longest in situ CO$_2$ measurement record in the Southern Hemisphere, and second longest globally, and has applicability in a wide range of carbon cycle studies. Consistent with original goals, Baring Head has proved to be a good location for observing clean

marine boundary-layer air arriving from the high-latitude Southern Ocean that has been isolated from contact with land for extended durations of time. Depending on air-mass history, atmospheric CO_2 at Baring Head responds to processes on local to global scales, and one of the advantages of a continuous record is that we can carefully filter the data for clean background air conditions (Fig. 3).

We have used the filtered steady period time series for comparisons to the background stations South Pole and Mauna Loa from the SIO network, and to atmospheric model simulations. These comparisons reveal a seasonal cycle that results from a combination of Northern Hemisphere and Southern Hemisphere land and ocean influences and is sensitive to interhemispheric transport. Interannual variations in atmospheric CO_2 growth rate at Baring Head are strongly correlated with ENSO, reflecting tropical and possibly Southern Ocean carbon cycle responses. The multidecadal trends at Baring Head follow those at South Pole closely throughout the record, with a suggestion of a possible divergence by $+0.3$ ppm/decade since 2001. The differences with respect to Mauna Loa grow steadily in response to increasing emissions in the Northern Hemisphere and ocean uptake in the Southern Hemisphere, and do not appear to be leveling off as might be expected if Southern Ocean uptake efficiency were reducing dramatically.

To date, the impact of the proposed $0.1 \, \mathrm{Pg \, C \, yr^{-1}}$ decade^{-1} Southern Ocean flux changes (Le Quéré et al., 2007) on atmospheric gradients is below detection limits, given uncertainties in comparing CO_2 records from independent stations and laboratories and the limited number of atmospheric CO_2 stations in the Southern Hemisphere. Our ability to detect and monitor changes in Southern Ocean carbon fluxes could be advanced by improved compatibility between sites and laboratories to the 0.05 ppm level long recommended by WMO (WMO, 2011; 2012) and by a significantly expanded observing network. At present, this ability is critically dependent on the continuation of the few existing long time series of atmospheric CO_2, such as that from Baring Head. Aspects of this record, including (1) the seasonal cycle, (2) interannual variations in the seasonal cycle, (3) the growth rate relationship with ENSO, (4) the non-ENSO related interannual variability, (5) the long-term trends with respect to South Pole and Mauna Loa, and (6) changes in these long-term trends, can provide important data-based tests of coupled atmosphere-ocean models and their ability to accurately represent the effects of climate change on Southern Ocean carbon cycling. We encourage the continued use of the Baring Head atmospheric CO_2 record in such efforts.

References

Bacastow, R. B.: Modulation of atmospheric carbon-dioxide by the Southern Oscillation, Nature, 261, 116–118, doi:10.1038/261116a0, 1976.

Baker, D. F., Law, R. M., Gurney, K. R., Rayner, P., Peylin, P., Denning, A. S., Bousquet, P., Bruhwiler, L., Chen, Y.-H., Ciais, P., Fung, I. Y., Heimann, M., John, J., Maki, T., Maksyutov, S., Masarie, K., Prather, M., Pak, B., Taguchi, S., and Zhu, Z.: TransCom 3 inversion intercomparison: Impact of transport model errors on the interannual variability of regional CO_2 fluxes, 1988–2003, Global Biogeochem. Cycles, 20, GB1002, doi:10.1029/2004GB002439, 2006.

Boden, T. A., Marland, G., and Andres, R. J.: Global, Regional, and National Fossil-Fuel CO_2 Emissions, Carbon Dioxide Information Analysis Center, Oak Ridge National Laboratory, U.S. Department of Energy, doi:10.3334/CDIAC/00001, Oak Ridge, Tenn., U.S.A., 2009.

Böning, C. W., Dispert, A., Visbeck, M., Rintoul, S. R., and Schwarzkopf, F. U.: The response of the Antarctic Circumpolar Current to recent climate change, Nat. Geosci., 1, 864–869, doi:10.1038/ngeo362, 2008.

Brailsford, G. W., Stephens, B. B., Gomez, A. J., Riedel, K., Mikaloff Fletcher, S. E., Nichol, S. E., and Manning, M. R.: Long-term continuous atmospheric CO_2 measurements at Baring Head, New Zealand, Atmos. Meas. Tech., 5, 3109–3117, doi:10.5194/amt-5-3109-2012, 2012.

Butler, A. H., Thompson, D. W. J., and Gurney, K. R.: Observed relationships between the Southern Annular Mode and atmospheric carbon dioxide, Global Biogeochem. Cycles, 21, GB4014, doi:10.1029/2006GB002796, 2007.

Caldeira, K. and Duffy, P. B.: The role of the Southern Ocean in uptake and storage of anthropogenic carbon dioxide, Science, 287, 620–622, doi:10.1126/science.287.5453.620, 2000.

Cleveland, R. B., Cleveland, W. S., McRae, J. E., and Terpenning, I.: STL: A seasonal-trend decomposition procedure based on loess, J. Official Statistics, 6, 3–73, 1990.

Cleveland, W. S. and McRae, J. E.: The use of loess and STL in the analysis of atmospheric CO_2 and related data., in: The Statistical Treatment of CO_2 Data Records, edited by: Elliot, W. P., National Oceanic and Atmospheric Administration, Silver Springs, Maryland., 61–81, 1989.

Dargaville, R. J., Heimann, M., McGuire, A. D., Prentice, I. C., Kicklighter, D. W., Joos, F., Clein, J. S., Esser, G., Foley, J., Kaplan, J., Meier, R. A., Melillo, J. M., Moore, B., Ramankuty, N., Reichenau, T., Schloss, A., Sitch, S., Tian, H., Williams, L. J., and Wittenberg, U.: Evaluation of terrestrial carbon cycle models with atmospheric CO_2 measurements: Results from transient simulations considering increasing CO_2, climate, and land-use effects, Glob. Biogeochem. Cycles, 16, 1092, doi:10.1029/2001GB001426, 2002.

Dargaville, R. J., Doney, S. C., and Fung, I. Y.: Inter-annual variability in the interhemispheric atmospheric CO_2 gradient: contributions from transport and the seasonal rectifier, Tellus B, 711–722, doi:10.1034/j.1600-0889.2003.00038.x, 2003.

Erickson, D. J., Rasch, P. J., Tans, P. P., Friedlingstein, P., Ciais, P., Maier-Reimer, E., Six, K., Fischer, C. A., and Walters, S.: The seasonal cycle of atmospheric CO_2: A study based on the NCAR Community Climate Model (CCM2), J. Geophys. Res., 101, 15079–15097, doi:10.1029/95JD03680, 1996.

Feely, R., Wanninkhof, R., Takahashi, T., and Tans, P.: Influence of El Niño on the equatorial Pacific contribution to atmospheric CO_2 accumulation, Nature, 398, 597–601, doi:10.1038/19273, 1999.

Friedlingstein, P., Cox, P., Betts, R., Bopp, L., Von Bloh, W., Brovkin, V., Cadule, P., Doney, S., Eby, M., Fung, I., Bala, G., John, J., Jones, C., Joos, F., Kato, T., Kawamiya, M., Knorr, W., Lindsay, K., Matthews, H. D., Raddatz, T., Rayner, P., Reick, C., Roeckner, E., Schnitzler, K. -., Schnur, R., Strassmann, K., Weaver, A. J., Yoshikawa, C., and Zeng, N.: Climate-carbon cycle feedback analysis: Results from the C⁴MIP model intercomparison, J. Clim., 19, 3337–3353, doi:10.1175/JCLI3800.1, 2006.

Globalview-CO2: Cooperative Atmospheric Data Integration Project - Carbon Dioxide, CD-ROM, NOAA ESRL, Boulder, Colorado, [Also available on internet via anonymous FTP to ftp.cmdl.noaa.gov, Path: ccg/co2/GLOBALVIEW], 2011.

Gordon, N. D.: Computer-derived air trajectories, Scientific Report 22, New Zealand Meteorological Service, Wellington, New Zealand, 1–13, 1986.

Gruber, N., Gloor, M., Fletcher, S. E. M., Doney, S. C., Dutkiewicz, S., Follows, M. J., Gerber, M., Jacobson, A. R., Joos, F., Lindsay, K., Menemenlis, D., Mouchet, A., Mueller, S. A., Sarmiento, J. L., and Takahashi, T.: Oceanic sources, sinks, and transport of atmospheric CO_2, Global Biogeochem. Cycles, 23, GB1005, doi:10.1029/2008GB003349, 2009.

Gu, L., Baldocchi, D., Verma, S. B., Black, T. A., Vesala, T., Falge, E. M., and Dowty, P. R.: Advantages of diffuse radiation for terrestrial ecosystem productivity, J. Geophys. Res., 107, 4050, doi:10.1029/2001JD001242, 2002.

Gurney, K. R., Law, R. M., Denning, A. S., Rayner, P. J., Baker, D., Bousquet, P., Bruhwiler, L., Chen, Y.-H., Ciais, P., Fan, S., Fung, I. Y., Gloor, M., Heimann, M., Higuchi, K., John, J., Maki, T., Maksyutov, S., Masarie, K., Peylin, P., Prather, M., Pak, B. C., Randerson, J., Sarmiento, J., Taguchi, S., Takahashi, T., and Yuen, C.-W.: Towards robust regional estimates of CO_2 sources and sinks using atmospheric transport models, Nature, 415, 626–630, doi:10.1038/415626a, 2002.

Gurney, K. R., Law, R. M., Denning, A. S., Rayner, P. J., Baker, D., Bousquet, P., Bruhwiler, L., Chen, Y.-H., Ciais, P., Fan, S., Fung, I. Y., Gloor, M., Heimann, M., Higuchi, K., John, J., Kowalczyk, E., Maki, T., Maksyutov, S., Peylin, P., Prather, M., Pak, B. C., Sarmiento, J., and Taguchi, S.: Transcom 3 CO_2 Inversion Intercomparison: 1. Annual mean control results and sensitivity to transport and prior flux information, Tellus B, 55, 555–579, doi:10.1034/j.1600-0889.2003.00049.x, 2003.

Gurney, K. R., Law, R. M., Denning, A. S., Rayner, P. J., Pak, B. C., Baker, D., Bousquet, P., Bruhwiler, L., Chen, Y.-H., Ciais, P., Fung, I. Y., Heimann, M., John, J., Maki, T., Maksyutov, S., Peylin, P., Prather, M., and Taguchi, S.: Transcom 3 inversion intercomparison: Model mean results for the estimation of seasonal carbon sources and sinks, Global Biogeochem. Cycles, 18, GB1010, doi:10.1029/2003GB002111, 2004.

Gurney, K. R., Baker, D., Rayner, P., and Denning, S.: Interannual variations in continental-scale net carbon exchange and sensitivity to observing networks estimated from atmospheric CO_2 inversions for the period 1980 to 2005, Global Biogeochem. Cycles, 22, GB3025, doi:10.1029/2007GB003082, 2008.

Hall, A. and Visbeck, M.: Synchronous variability in the southern hemisphere atmosphere, sea ice, and ocean resulting from the annular mode, J. Climate, 15, 3043-3057, doi:10.1175/1520-0442(2002)015<3043:SVITSH>2.0.CO;2, 2002.

Hashimoto, H., Nemani, R., White, M., Jolly, W., Piper, S., Keeling, C., Myneni, R., and Running, S.: El Niño-Southern Oscillation-induced variability in terrestrial carbon cycling, J. Geophys. Res., 109, D23110, doi:10.1029/2004JD004959, 2004.

Heimann, M. and Keeling, C. D.: A three-dimensional model of atmospheric CO_2 transport based on observed winds: 2. Model description and simulated tracer experiments, in: Geophysical Monograph 55, Aspects of climate variability in the Pacific and the Western Americas, edited by: Peterson, D. H., American Geophysical Union, Washington DC., 237–275, doi:10.1029/GM055p0237, 1989.

Heimann, M., Esser, G., Haxeltine, A., Kaduk, J., Kicklighter, D. W., Knorr, W., Kohlmaier, G. H., McGuire, A. D., Melillo, J., Moore, B., Otto, R. D., Prentice, I. C., Sauf, W., Schloss, A., Sitch, S., Wittenberg, U., and Wurth, G.: Evaluation of terrestrial Carbon Cycle models through simulations of the seasonal cycle of atmospheric CO_2: First results of a model intercomparison study, Global Biogeochem. Cycles, 12, 1–24, doi:10.1029/97GB01936, 1998.

Heimann, M. and Körner, S.: The global atmospheric tracer model TM3, in Max-Planck-Institut für Biogeochemie (Eds.): Technical Report, Vol. 5, Max-Planck-Institut für Biogeochemie, Jena, Germany, 131 pp., 2003.

IPCC: Contribution of Working Group I to the Fourth Assessment Report of the Intergovernmental Panel on Climate Change, Cambridge University Press, Cambridge, United Kingdom and New York, NY, USA., 2007.

Jones, C., Collins, M., Cox, P. and Spall, S.: The carbon cycle response to ENSO: A coupled climate-carbon cycle model study, J. Climate, 14, 4113–4129, doi:10.1175/1520-0442(2001)014<4113:TCCRTE>2.0.CO;2, 2001.

Kalnay, E. C., Kanamitsu, M., Kistler, R., Collins, W., Deaven, D., Gandin, L., Iredell, M., Saha, S., White, G.,Woollen, J., Zhu, Y., Chellian, M., Ebisuzaki, W., Higgins, W., Janowiak, J., Mo, K. C., Ropelewski, C., Wang, J., Leetmaa, A., Reynolds, R., Jenne, R., and Joseph, D.: The NCEP/NCAR 40-year reanalysis project, B. Am. Meteorol. Soc., 77, 347–471, doi:10.1175/1520-0477(1996)077<0437:TNYRP>2.0.CO;2, 1996.

Kawa, S., Erickson, D., Pawson, S., and Zhu, Z.: Global CO_2 transport simulations using meteorological data from the NASA data assimilation system, J. Geophys. Res., 109, D18312, doi:10.1029/2004JD004554, 2004.

Keeling, C. D.: The concentration and isotopic abundances of carbon dioxide in rural and marine air, Geochem. Cosmochem. Acta, 24, 277–298, doi:10.1016/0016-7037(61)90023-0, 1961.

Keeling, C. D., Bacastow, R. B., Carter, A. F., Piper, S. C., Whorf, T. P., Heimann, M., Mook, W. G., and Roeloffzen, H.: A three dimensional model of atmospheric CO_2 transport based on observed winds: 1. Analysis of observational data, in: Geophysical Monograph 55, Aspects of climate variability in the Pacific and the Western Americas, edited by: Peterson, D. H., American Geophysical Union, Washington D.C., 165–236, doi:10.1029/GM055p0165, 1989a.

Keeling, C. D., Piper, S. C., and Heimann, M.: A three-dimensional model of atmospheric CO_2 transport based on observed winds: 4. Mean annual gradients and interannual variations, in: Geophysical Monograph 55, Aspects of climate variability in the Pacific and the Western Americas, edited by: Peterson, D. H., American Geophysical Union, Washington D. C., 305–363, doi:10.1029/GM055p0305, 1989b.

Keeling, C. D., Piper, S. C., Bacastow, R. B., Wahlen, M., Whorf, T. P., Heimann, M., and Meijer, H. A.: Exchanges of atmospheric CO_2 and $^{13}CO_2$ with the terrestrial biosphere and oceans from 1978 to 2000. I. Global aspects, Scripps Institution of Oceanography, San Diego, 2001.

Kidson, J. W.: An automated procedure for the identification of synoptic types applied to the New Zealand region, Int. J. Climatol., 14, 711–721, doi:10.1002/joc.3370140702, 1994.

Kidson, J.: An analysis of New Zealand synoptic types and their use in defining weather regimes, Int. J. Climatol., 20, 299–316, doi:10.1002/(SICI)1097-0088(20000315)20:3<299::AID-JOC474>3.0.CO;2-B, 2000.

Knox, F. and McElroy, M. B.: Changes in atmospheric CO_2 : influence of the marine biota at high latitude, J. Geophys. Res., Wash., D.C, 89, 4629–4637, doi:10.1029/JD089iD03p04629, 1984.

Law, R. M. Chen, Y.-H., Gurney, K. R., and Transcom 3 modellers: Transcom 3 CO_2 Inversion Intercomparison: 2. Sensitivity of annual mean results to data choices, Tellus B, 580–595, doi:10.1034/j.1600-0560.2003.00053.x, 2003.

Law, R. M., Matear, R. J., and Francey, R. J.: Comment on "Saturation of the Southern Ocean CO_2 sink due to recent climate change", Science, 319, 570, doi:10.1126/science.1149077, 2008.

Le Quéré, C., Aumont, O., Bopp, L., Bousquet, P., Ciais, P., Francey, R., Heimann, M., Keeling, C. D., Keeling, R. F., Kheshgi, H., Peylin, P., Piper, S. C., Prentice, I. C., and Rayner, P. J.: Two decades of ocean CO_2 sink and variability, Tellus B, 55, 649–656, doi: 10.1034/j.1600-0889.2003.00043.x, 2003.

Le Quéré, C., Rödenbeck, C., Buitenhuis, E. T., Conway, T. J., Langenfelds, R., Gomez, A., Labuschagne, C., Ramonet, M., Nakazawa, T., Metzl, N., Gillett, N., and Heimann, M.: Saturation of the Southern Ocean CO_2 Sink due to recent climate change, Science, 316, 1735, doi:10.1126/science.1136188, 2007.

Lenton, A. and Matear, R. J.: Role of the Southern Annular Mode (SAM) in Southern Ocean CO_2 uptake, Global Biogeochem. Cycles, 21, GB2016, doi:10.1029/2006GB002714, 2007.

Lenton, A., Codron, F., Bopp, L., Metzl, N., Cadule, P., Tagliabue, A., and Le Sommer, J.: Stratospheric ozone depletion reduces ocean carbon uptake and enhances ocean acidification, Geophys. Res. Lett., 36, L12606, doi:10.1029/2009GL038227, 2009.

Louanchi, F. and Hoppema, M.: Interannual variations of the Antarctic Ocean CO_2 uptake from 1986 to 1994, Mar. Chem., 72, 103–114, doi:10.1016/S0304-4203(00)00076-1, 2000.

Lovenduski, N. S., Gruber, N., Doney, S. C., and Lima, I. D.: Enhanced CO_2 outgassing in the Southern Ocean from a positive phase of the Southern Annular Mode, Global Biogeochem. Cycles, 21, doi:10.1029/2006GB002900, 2007.

Lovenduski, N. S. and Ito, T.: The future evolution of the Southern Ocean CO_2 sink, J. Mar. Res., 67, 597–617, doi:10.1357/002224009791218832, 2009.

Lowe, D. C., Guenther, P. R., and Keeling, C. D.: The concentration of atmospheric carbon dioxide at Baring Head, New Zealand, Tellus, 31, 58–67, 1979.

Manning, M. R. and Pohl, K. P.: Atmospheric carbon dioxide monitoring in New Zealand, 1971–1985, DSIR, Institute of Nuclear Sciences, Lower Hutt, New Zealand, http://webcat.niwa.co.nz/documents/INS-R-350.pdf, (last access: August 2012), 1986.

Manning, M. R., Gomez, A. J. and Pohl, K. P.: Atmospheric CO_2 record from in situ measurements at Baring Head, in: Trends '93: A Compendium of Data on Global Change, ORNL/CDIAC-65, edited by: Boden, T. A., Kaiser, D. P., Sepanski, R. J., and Stoss, F. W., Oak Ridge, Tenn., U.S.A., 1994.

Marshall, G.: Trends in the southern annular mode from observations and reanalyses, J. Climate, 16, 4134–4143, http://dx.doi.org/10.1175/1520-0442(2003)016$($4134:TITSAM$)$2.0.CO;2, 2003.

Masarie, K. A., Petron, G., Andrews, A., Bruhwiler, L., Conway, T. J., Jacobson, A. R., Miller, J. B., Tans, P. P., Worthy, D. E., and Peters, W.: Impact of CO_2 measurement bias on CarbonTracker surface flux estimates, J. Geophys. Res., 116, D17305, doi:10.1029/2011JD016270, 2011.

Mercado, L. M., Bellouin, N., Sitch, S., Boucher, O., Huntingford, C., Wild, M., and Cox, P. M.: Impact of changes in diffuse radiation on the global land carbon sink, Nature, 458, 1014–1017, doi:10.1038/nature07949, 2009.

Metzl, N.: Decadal increase of oceanic carbon dioxide in Southern Indian Ocean surface waters (1991-2007), Deep-Sea Res. Pt. II, 56, 607–619, doi:10.1016/j.dsr2.2008.12.007, 2009.

Mullan, B.: Effects of ENSO on New Zealand and the South Pacific, in: Prospects and needs for climate forecasting , Miscellaneous Series 34, edited by: Braddock, D., Royal Society of New Zealand, Wellington, New Zealand., 23–27, 1996.

Nevison, C. D., Mahowald, N. M., Doney, S. C., Lima, I. D., Van der Werf, G. R., Randerson, J. T., Baker, D. F., Kasibhatla, P., and McKinley, G. A.: Contribution of ocean, fossil fuel, land biosphere, and biomass burning carbon fluxes to seasonal and in-

terannual variability in atmospheric CO$_2$, J. Geophys. Res., 113, G01010, doi:10.1029/2007JG000408, 2008.

Page, S., Siegert, F., Rieley, J., Boehm, H., Jaya, A., and Limin, S.: The amount of carbon released from peat and forest fires in Indonesia during 1997, Nature, 420, 61–65, doi:10.1038/nature01131, 2002.

Patra, P. K., Law, R. M., Peters, W., Rödenbeck, C., Takigawa, M., Aulagnier, C., Baker, I., Bergmann, D. J., Bousquet, P., Brandt, J., Bruhwiler, L., Cameron-Smith, P. J., Christensen, J. H., Delage, F., Denning, A. S., Fan, S., Geels, C., Houweling, S., Imasu, R., Karstens, U., Kawa, S. R., Kleist, J., Krol, M. C., Lin, S. -., Lokupitiya, R., Maki, T., Maksyutov, S., Niwa, Y., Onishi, R., Parazoo, N., Pieterse, G., Rivier, L., Satoh, M., Serrar, S., Taguchi, S., Vautard, R., Vermeulen, A. T., and Zhu, Z.: TransCom model simulations of hourly atmospheric CO$_2$: Analysis of synoptic-scale variations for the period 2002–2003, Global Biogeochem. Cycles, 22, GB4013, doi:10.1029/2007GB003081, 2008.

Pearman, G. I. and Hyson, P.: Activities of the global biosphere as reflected in atmospheric CO$_2$ records, J. Geophys. Res., 85, 4457–4467, doi:10.1029/JC085iC08p04457, 1980.

Peters, W., Jacobson, A. R., Sweeney, C., Andrews, A. E., Conway, T. J., Masarie, K., Miller, J. B., Bruhwiler, L. M. P., Petron, G., Hirsch, A. I., Worthy, D. E. J., van der Werf, G. R., Randerson, J. T., Wennberg, P. O., Krol, M. C. ,and Tans, P. P.: An atmospheric perspective on North American carbon dioxide exchange: CarbonTracker, P. Natl. Acad. Sci. USA., 104, 18925–18930, doi:10.1073/pnas.0708986104, 2007.

Reichenau, T. and Esser, G.: Is interannual fluctuation of atmospheric CO$_2$ dominated by combined effects of ENSO and volcanic aerosols?, Global Biogeochem. Cycles, 17, 1094, doi:10.1029/2002GB002025, 2003.

Rödenbeck, C., Houweling, S., Gloor, M., and Heimann, M.: CO$_2$ flux history 1982–2001 inferred from atmospheric data using a global inversion of atmospheric transport, Atmos. Chem. Phys., 3, 1919–1964, doi:10.5194/acp-3-1919-2003, 2003.

Rödenbeck, C., Conway, T. J., and Langenfelds, R. L.: The effect of systematic measurement errors on atmospheric CO$_2$ inversions: a quantitative assessment, Atmos. Chem. Phys., 6, 149–161, doi:10.5194/acp-6-149-2006, 2006.

Roy, T., Rayner, P., Matear, R. and Francey, R.: Southern hemisphere ocean CO$_2$ uptake: reconciling atmospheric and oceanic estimates, Tellus B, 701–710, doi:10.1034/j.1600-0889.2003.00058.x, 2003.

Saenko, O., Fyfe, J., and England, M.: On the response of the oceanic wind-driven circulation to atmospheric CO$_2$ increase, Clim. Dynam., 25, 415–426, doi:10.1007/s00382-005-0032-5, 2005.

Sarmiento, J. L. and Toggweiler, J. R.: New model for the role of the oceans in determining atmospheric PCO$_2$, Nature, 308, 621–624, doi:10.1038/308621a0, 1984.

Sarmiento, J. L., Hughes, T. M. C., Stouffer, R. J., and Manabe, S.: Simulated response of the ocean carbon cycle to anthropogenic climate warming, Nature, 393, 245–249, doi:10.1038/30455, 1998.

Siegenthaler, U. and Wenk, T.: Rapid atmospheric CO$_2$ variations and ocean circulation, Nature, 308, 624–626, doi:10.1038/308624a0, 1984.

Stephens, B. B., Gurney, K. R., Tans, P. P., Sweeney, C., Peters, W., Bruhwiler, L., Ciais, P., Ramonet, M., Bousquet, P., Nakazawa, T., Aoki, S., Machida, T., Inoue, G., Vinnichenko, N., Lloyd, J., Jordan, A., Heimann, M., Shibistova, O., Langenfelds, R. L., Steele, L. P., Francey, R. J., and Denning, A. S.: Weak northern and strong tropical land carbon uptake from vertical profiles of atmospheric CO$_2$, Science, 316, 1732, doi:10.1126/science.1137004, 2007.

Takahashi, T., Sutherland, S. C., Wanninkhof, R., Sweeney, C., Feely, R. A., Chipman, D. W., Hales, B., Friederich, G., Chavez, F., Sabine, C., Watson, A., Bakker, D. C. E., Schuster, U., Metzl, N., Yoshikawa-Inoue, H., Ishii, M., Midorikawa, T., Nojiri, Y., Koertzinger, A., Steinhoff, T., Hoppema, M., Olafsson, J., Arnarson, T. S., Tilbrook, B., Johannessen, T., Olsen, A., Bellerby, R., Wong, C. S., Delille, B., Bates, N. R., and de Baar, H. J. W.: Climatological mean and decadal change in surface ocean pCO$_2$, and net sea-air CO$_2$ flux over the global oceans, Deep-Sea Res. Pt. II, 56, 554–577, doi:10.1016/j.dsr2.2008.12.009, 2009.

Thompson, D. W. J. and Solomon, S.: Interpretation of recent Southern Hemisphere climate change, Science, 296, 895, doi:10.1126/science.1069270, 2002.

Verdy, A., Dutkiewicz, S., Follows, M. J., Marshall, J., and Czaja, A.: Carbon dioxide and oxygen fluxes in the Southern Ocean: Mechanisms of interannual variability, Global Biogeochem. Cycles, 21, GB2020, doi:10.1029/2006GB002916, 2007.

Wetzel, P., Winguth, A., and Maier-Reimer, E. : Sea-to-air CO$_2$ flux from 1948 to 2003: A model study, Glob. Biogeochem. Cycles, 19, GB2005, doi:10.1029/2004GB002339, 2005.

WDCGG: DVD No. 4, WMO World Data Centre for Greenhouse Gases, Tokyo, Japan, http://ds.data.jma.go.jp/gmd/wdcgg/pub/products/cd-rom/dvd_04, 2012.

WMO: Report of the 15th WMO/IAEA Meeting of Experts on Carbon Dioxide, Other Greenhouse Gases and Related Tracers Measurement Techniques, edited by: Brand, W., WMO TD No. 1553, Jena, Germany, 2011.

WMO: Report of the 16th WMO/IAEA Meeting on Carbon Dioxide, Other Greenhouse Gases, and Related Measurement Techniques (GGMT-2011), edited by: Brailsford, G., GAW Report 206, Wellington, New Zealand, 2012.

Wolter, K. and Timlin, M. S.: Monitoring ENSO in COADS with a seasonally adjusted principal component index. Proc. of the 17th Climate Diagnostics Workshop, Norman, OK, NOAA/NMC/CAC, NSSL, Oklahoma Clim. Survey, CIMMS and the School of Meteor., Univ. of Oklahoma, 52–57, 1993.

Zeng, N., Mariotti, A., and Wetzel, P.: Terrestrial mechanisms of interannual CO$_2$ variability, Global Biogeochem. Cycles, 19, GB1016, doi:10.1029/2004GB002273 2005.

Zickfeld, K., Fyfe, J. C., Eby, M., and Weaver, A. J.: Comment on "Saturation of the Southern Ocean CO$_2$ Sink Due to Recent Climate Change", Science, 319, 570, doi:10.1126/science.1146886, 2008.